PROCEEDINGS of the
23rd International Congress on Acoustics
9 to 13 September 2019 in Aachen, Germany

On the Directional Properties of Energy Decay Curves

Marco BERZBORN[(1)], Mélanie NOLAN[(2,3)], Efren FERNANDEZ-GRANDE[(2)], Michael VORLÄNDER[(1)]

[(1)]Institute of Technical Acoustics, RWTH Aachen University, Kopernikusstr. 5, 52074 Germany, mbe@akustik.rwth-aachen.de
[(2)]Acoustic Technology, Department of Electrical Engineering, Technical University of Denmark, 2800 Kgs. Lyngby, Denmark
[(3)]Saint-Gobain Ecophon, 265 75 Hyllinge, Sweden

Abstract
A prerequisite for the absorption coefficient estimation in accordance with ISO 354 is that the sound field in the used reverberation room is diffuse. A diffuse sound field is generally defined by the isotropy condition – requiring the sound field to be composed of infinitely many sound waves from uncorrelated sources with directions of arrival uniformly distributed over a sphere. Microphone arrays allow for the decomposition of the sound field into a continuum of plane waves composing it and therefore directly allow for the analysis of the isotropy condition. By extending this concept to the decay process of the sound field we propose the directional energy decay curve as an analysis framework of the directional properties of the decaying sound field in a reverberation room.
Keywords: Diffuseness, Isotropy, Reverberation Rooms, Spherical Arrays

1 INTRODUCTION

Knowledge of the acoustic absorption properties of materials is crucial in the fields of architectural and room acoustics simulations. The random-incidence absorption coefficient is measured according to the international standard ISO-354 [1] in a reverberation room with the prerequisite of the sound field in the room being diffuse. However, studies showed high uncertainties in the method and a poor inter-laboratory reproducibility of the results [2]. It is assumption that these problems are in part caused by a non-diffuse sound field [3]. A standardized robust metric for the characterization or calibration of reverberation rooms, however, is currently lacking [4].
The fundamental definition is that the diffuse sound field is isotropic – requiring the sound field to be composed of infinitely many sound waves from uncorrelated sources with directions of arrival (DOAs) uniformly distributed over a sphere [5–7]. Important consequences for sound fields in rooms are a uniform sound pressure distribution over space in the room and a uniform hemispherical energy distribution over an absorber specimen in a reverberation room [1, 5]. The two latter points are prerequisites for the application of Sabine's equation for the calculation of the absorption coefficient [1, 3].
Thiele [8] and Gover [7] discuss the distribution and directional variation of the incident energy measured with a directional receiver in a room to study the isotropy of a sound field in steady state. More recently, Nolan et al. [6] studied the isotropy conditions of the steady state sound field in reverberation rooms using a spherical harmonic expansion of the wave number spectrum. Earlier studies by Hunt et al. [9] and Kuttruff [10] pointed out the influence of the absorbing sample on the decay process of the sound field and the resulting multi-exponential nature of the corresponding energy decay curves (EDCs). This paper extends on the works by Thiele [8] and Gover [7] by analyzing the directional properties of the sound field during the decay process based on the directional energy decay curve (DEDC) which we calculate by applying the Schroeder integration [11] on a plane wave decomposition of the sound field, while the aforementioned studies were limited to the steady state sound field as well as time windows of single reflections in room impulse responses.
Section 2 introduces the framework for the directional decomposition of the sound field using a spherical microphone array (SMA), as well as the concept and calculation of the DEDC. Section 3 introduces the experimental setup under study in a reverberation room in different configurations with varying degrees of sound field isotropy. The results are presented in Section 4, followed by the conclusions in Section 5.

2 DIRECTIONAL ENERGY DECAY CURVE ANALYSIS

SMAs – or microphone arrays in general – allow for the capture of directional room impulse responses (DRIRs) retaining directional information about the sound field in the room [12] and, therefore, prove to be a viable tool in the analysis of sound field isotropy [6, 7].

2.1 Plane Wave Decomposition with Spherical Arrays

A DRIR measured with an SMA can be written as a vector of the microphone signals

$$\mathbf{p}(k) = [p(k, r, \theta_1, \phi_1), \ldots, p(k, r, \theta_L, \phi_L)]^{\mathrm{T}}, \tag{1}$$

where θ_l and ϕ_l are the elevation and azimuth angles of the l'th sensor position, respectively, k is the wave number, and $(.)^{\mathrm{T}}$ denotes the transpose operator. For a plane wave sound field we may write the sound pressure at the microphone positions of an SMA as [12]

$$\mathbf{p}(k) = \mathbf{B}(k)\mathbf{a_{nm}}(k), \tag{2}$$

where

$$\mathbf{B}(k) = \begin{pmatrix} b_0(k, r_1) Y_0^0(\theta_1, \phi_1) & b_1(k, r_1) Y_1^{-1}(\theta_1, \phi_1) & \cdots & b_N(k, r_1) Y_N^N(\theta_1, \phi_1) \\ b_0(k, r_2) Y_0^0(\theta_2, \phi_2) & b_1(k, r_2) Y_1^{-1}(\theta_2, \phi_2) & \cdots & b_N(k, r_2) Y_N^N(\theta_2, \phi_2) \\ \vdots & \vdots & \ddots & \vdots \\ b_0(k, r_L) Y_0^0(\theta_L, \phi_L) & b_1(k, r_L) Y_1^{-1}(\theta_L, \phi_L) & \cdots & b_N(k, r_L) Y_N^N(\theta_L, \phi_L) \end{pmatrix}, \tag{3}$$

with the spherical harmonic basis functions[1] $Y_n^m(\theta_l, \phi_l)$ of order n and degree m evaluated at the elevation and azimuth angles, respectively, and the modal strength function $b_n(k, r_l)$ for an open array, both with a maximum spherical harmonic (SH) order N. The vector $\mathbf{a_{nm}}(\mathbf{k})$ contains the SH coefficients defining the amplitude density function of the plane waves composing the sound field. For a single plane wave incident this becomes a vector containing the SH basis functions evaluated at the DOA. Applying plane wave decomposition, we decompose the sound field into a continuum of plane waves, yielding the plane wave amplitude density function in the spatial domain, also referred to as the wave number spectrum [12]

$$a(k, \theta_q, \phi_q) = \frac{4\pi}{(N+1)^2} \mathbf{y}^{\mathrm{T}}(\theta_q, \phi_q) \mathbf{B}^{\dagger}(k) \mathbf{p}(k), \tag{4}$$

where $\mathbf{y}^{\mathrm{T}}(\theta_q, \phi_q)$ is the steering vector of the array containing the SH basis functions evaluated at the q'th steering direction defined by the angles (θ_q, ϕ_q). The $(.)^{\dagger}$ operator denotes the Moore-Penrose Pseudo-inverse. Applying the inverse discrete Fourier transform we can calculate the time domain plane wave amplitude density $a(t, \theta_q, \phi_q)$ which is to be interpreted as the angular distribution of plane waves impinging on the receiver over time.

2.2 Directional Energy Decay Curves

The EDC is a fundamental tool in the analysis of sound fields in rooms, providing information about the energy decay of a steady state sound field in a room excited by broadband noise [3]. Schroeder [11] proposed the calculation of the EDC by an integration of the squared room impulse response (RIR). Analogously, we define the DEDC by performing the Schroeder integration on the amplitude density function from Eq. (4), yielding

$$\begin{aligned} d(t, \theta_q, \phi_q) &= \int_t^{\infty} |a(\tau, \theta_q, \phi_q)|^2 d\tau \\ &= \int_0^{\infty} |a(\tau, \theta_q, \phi_q)|^2 d\tau - \int_0^t |a(\tau, \theta_q, \phi_q)|^2 d\tau = e(\theta_q, \phi_q) - \int_0^t |a(\tau, \theta_q, \phi_q)|^2 d\tau, \end{aligned} \tag{5}$$

[1] We use real valued SH basis functions following the Ambix phase convention and N3D normalization.

where $e(\theta_q, \phi_q)$ is the steady state energy arriving from a single discrete direction (θ_q, ϕ_q). In contrast to the directional analysis of sound fields purely based on DRIRs – which may only give information about the directional distribution of energy for a single snapshot in time – the analysis of the DEDC provides directional information about the decay process and the angular distribution of the remaining energy for each point in time. It consequently allows to reveal non-uniform energy decays and may highlight directions with dominant energy incidence. A remark that needs to be made is that the definition of the DEDC here does not allow for a strict angular separation of individual decaying modes but rather a frequency band of multiple modes with arbitrary mixing.

Gover [7] and Thiele [8] used the mean of absolute directional differences of the energy incidence from Q discrete directions

$$\sigma_e = \frac{1}{\langle e \rangle_\Omega} \sum_{q=1}^{Q} |e(\theta_q, \phi_q) - \langle e \rangle_\Omega|, \tag{6}$$

with the incident energy averaged over the direction of incidence $\Omega = (\theta_q, \phi_q)$

$$\langle e \rangle_\Omega = \frac{1}{Q} \sum_{q=1}^{Q} e(\theta_q, \phi_q), \tag{7}$$

to discuss the isotropy – they refer to it as directional diffusion – of a sound field in a room. In a similar fashion we may extend Eq. (6) to study the directional variation of the DEDC

$$\sigma_d(t) = \frac{1}{\langle d(t) \rangle_\Omega} \sum_{q=1}^{Q} |d(t, \theta_q, \phi_q) - \langle d(t) \rangle_\Omega|, \tag{8}$$

where $\langle d(t) \rangle_\Omega$ is the directional average of the DEDC over Ω at time instance t. Inserting Eq. (5) into Eq. (8) it may be seen that $\sigma_d(t=0) = \sigma_e$. Thiele [8] and Gover [7] further included a normalization factor calculated as in Eq. (6) for the case of a single plane wave, here referred to as $\sigma_{e,0}$. Analogously, we normalize Eq. (8) and apply a re-normalization by subtracting from one, yielding the estimated isotropy of the sound field,

$$\mu_d(t) = 1 - \frac{\sigma_d(t)}{\sigma_{e,0}}. \tag{9}$$

Equation (9) is a function in the interval $\mu_d(t) \in [0, 1]$, which will be zero for a single plane wave incident and one for a perfectly isotropic sound field.

For a more granular analysis we may also calculate the isotropy for the azimuth or elevation angle separately, which we denote as $\mu_{d,\phi}(t)$ and $\mu_{d,\phi}(t)$, respectively. To exemplary estimate the isotropy over elevation angles we first sum up the DEDC over the azimuth angle $d_{\Sigma,\phi}(t, \theta) = \sum_{u=1}^{U} d(t, \theta_q, \phi_u)$ before calculating the directional variation over the elevation $\langle d(t) \rangle_\theta = \frac{1}{Q} \sum_{q=1}^{Q} d_{\Sigma,\phi}(t, \theta_q)$, which we substitute into Eq. (8). It hast to be noted that the normalization term $\sigma_{e,0}$ also needs to be adjusted accordingly.

3 EXPERIMENTAL SETUP

The DEDCs were analyzed experimentally for a rectangular reverberation room at the Technical University of Denmark (2800 Kgs. Lyngby, Denmark) in four configurations: The empty room, with and without diffusing panels and the room occupied with an absorbing sample of glass wool with a flow resistivity of $12.9\,\mathrm{kPa \cdot s/m^2}$, a thickness of 100 mm and a surface area of $10.8\,\mathrm{m^2}$. The absorption coefficient of the absorbing sample is 1.04 for the 500 Hz third octave frequency band considered in this paper. The absorption values were measured according to ISO-354 [1] in the same room at an earlier time with mounted diffuser panels. The room has the dimensions $(x, y, z) = (6.25\,\mathrm{m}, 7.85\,\mathrm{m}, 4.9\,\mathrm{m})$ and an approximate volume of $245\,\mathrm{m^3}$ and a Schroeder frequency slightly over 300 Hz. The sound field in the room was excited by a source mounted in the corner below the

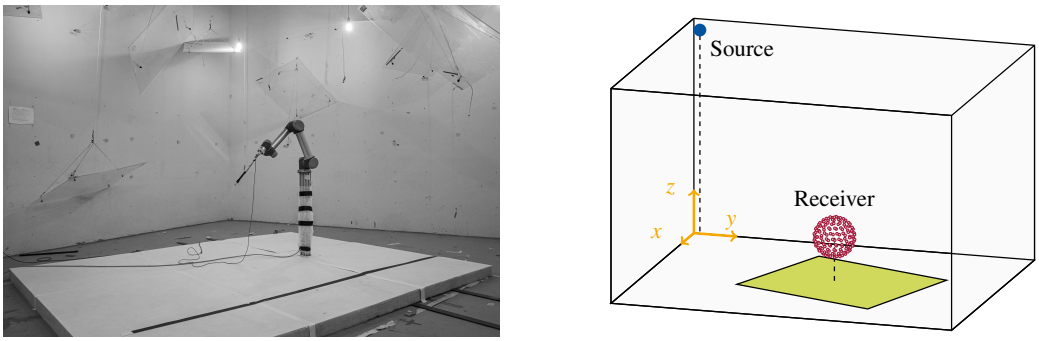

(a) (b)

Figure 1. The experimental setup with source and receiver positions as well as the absorber position in the reverberation room. The pose of the robotic arm in Fig. 1(a) marks the south pole of the inner sphere. For better visual interpretability only sampling positions on the outer sphere are shown in Fig. 1(b).

ceiling at approximately $(0.2\,\mathrm{m}, 0.2\,\mathrm{m}, 4.7\,\mathrm{m})$, cf. Fig. 1(b). The impulse response measurement was performed with the ITA-Toolbox [13] using exponential sweeps as excitation signal. The signal acquisition was performed using a National Instruments NI USB-4431 DAQmx system. An UR5 (Universal Robots, Odense, Denmark) scanning robot arm in combination with a pressure-field $1/2''$ Brüel & Kjær type 4192 microphone paired with a Brüel & Kjær Nexus pre-amplifier was used to sample a sequential dual-layer spherical microphone array, cf. Figs. 1(a) and 1(b). The two layers with radii $r = (0.25\,\mathrm{m}, 0.45\,\mathrm{m})$ consist of 144 sampling positions chosen according to an equal-area grid on the sphere [14]. Additional sampling positions inside the respective spheres were used to achieve good stabilization of the eigenfrequencies of the spheres [15]. The receiver array was centered at $(2.98\,\mathrm{m}, 4.16\,\mathrm{m}, 1\,\mathrm{m})$, cf. Fig. 1(b). The resulting virtual array consists of 310 sampling positions. For a SH order $N = 5$ this yields a usable frequency range of approximately 200 Hz - 3 kHz when fully equalizing for the modal strength of the array and thus ensuring a constant angular resolution [12]. For lower frequencies a soft limiting approach of the radial filter was used [16] to avoid degradation of the signal quality due to noise amplification. The used sequential array sampling approach provides a high signal-to-noise ratio and prevents microphone mismatch while minimizing potential positioning errors. The measurement duration for a full sequential array ranged from 2.5 h to 4.5 h depending whether an absorbing sample was present or not. The temperature was logged before and after each measurement. Temperature changes remained well below $0.3\,^{\circ}\mathrm{C}$ during the measurement of one sequential array.
Finally, the plane wave decomposition was performed for 882 steering directions chosen according to a Gaussian quadrature grid on a sphere [17]. The DEDCs were then calculated using the Schroeder integral after subtracting the measurement noise from the squared plane wave density function analogously to the noise subtraction method proposed by Chu [18]. The DEDCs were truncated to the shortest joint decay time corresponding to a decay of 50 dB ensuring decay curves with joint valid length.

4 RESULTS

Figures 2 to 5 show contour plots of the DEDCs for the four different configurations at time instances corresponding to the steady state sound field and decays of -5 dB, -10 dB, -15 dB, -25 dB, and -35 dB. The time instances are calculated from the zeroth-order spherical coefficient which corresponds to the omnidirectional response of the array. The DEDCs are normalized to the directional mean for each time instance and thus indicate variations from the mean energy incident over all directions. The estimated isotropy using Eq. (9) is given in Fig. 6, and in Fig. 7. Markers are placed at the same time instances as in Figs. 2 to 5.

Comparing Figs. 2 and 3 to Figs. 4 and 5 it is very apparent that the absorber has a strong influence on

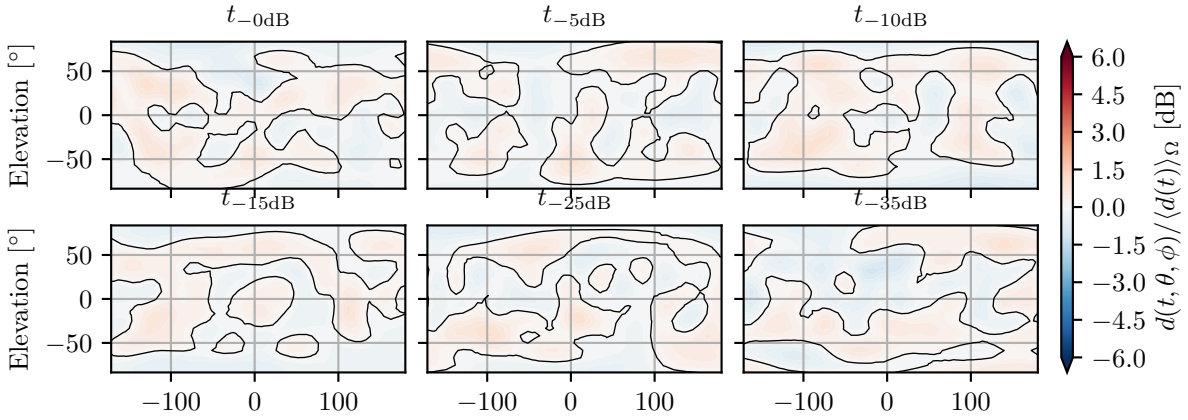

Figure 2. Normalized DEDC for the empty room with diffuser panels. Figures correspond to time instances with a omnidirectional energy decay of $[0,5,10,15,25,35]$ dB, respectively.

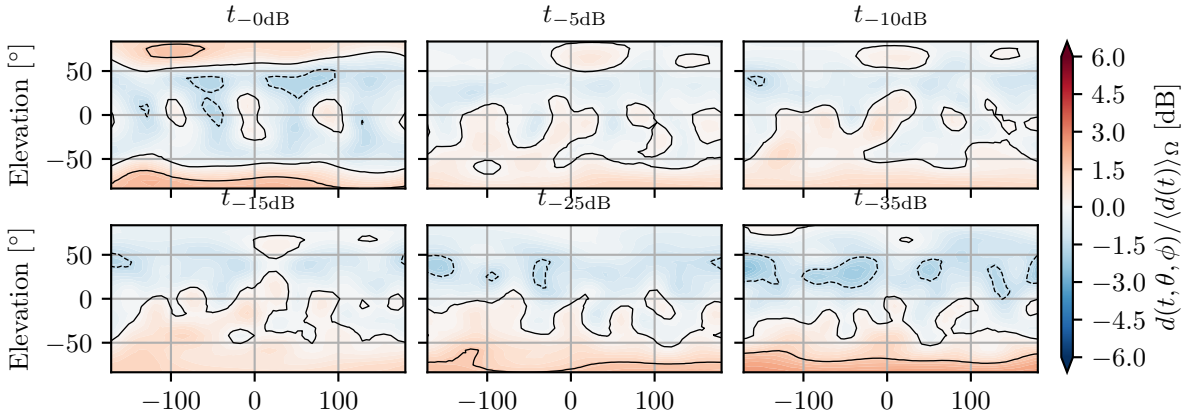

Figure 3. Normalized DEDC for the empty room without diffuser panels. Figures correspond to time instances with a omnidirectional energy decay of $[0,5,10,15,25,35]$ dB, respectively.

the sound field, as most energy in the lower hemisphere is absorbed. This consequently leads to a sound field which is not isotropic. This is reflected by a lower overall isotropy estimation for these cases compared to the cases without an absorbing sample, as seen in Fig. 6. While the sound field with the absorber present seems to be at least uniformly distributed over the upper hemisphere during the decay process when the diffuser panels are mounted in the room (cf. Fig. 4), one can observe a dominant concentration of energy in the equator region once the diffuser panels are removed, cf. Fig. 5. Despite a seemingly improved mixing of the sound field at $t_{-5\mathrm{dB}}$, and $t_{-10\mathrm{dB}}$, this effect increases with time, indicating an increase in energy flows tangential to the absorber for later times in the decay process. The maxima at azimuth angles $\phi = (-180°, -90°, 0°, 90°)$ are located in the direction of the sidewalls indicating that the decay process is dominated by normal modes corresponding to grazing incidence while oblique modes are not as pronounced. This may also be expected as the oblique modes are affected more by the absorber and consequently expected to decay faster. Accordingly, Fig. 6(b) shows a decrease in the estimated isotropy of the sound field for the later decay after it initially increased until $t_{-10\mathrm{dB}}$. This decrease is not found when diffuser panels are mounted in the room, in which case the estimated isotropy seems to converge to a constant value, cf. Fig. 6(b). From Fig. 7 it can be observed

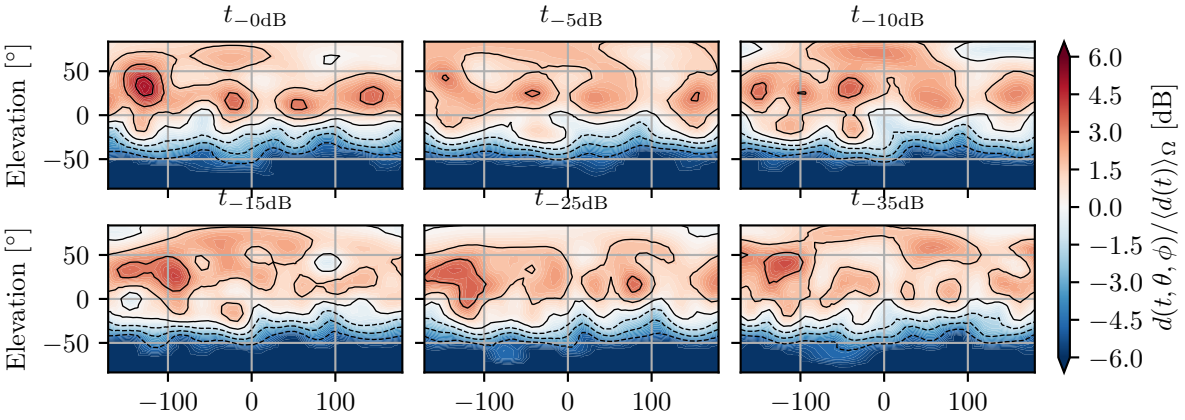

Figure 4. Normalized DEDC for the room with the absorber and with diffuser panels. Figures correspond to time instances with a omnidirectional energy decay of $[0, 5, 10, 15, 25, 35]$ dB, respectively.

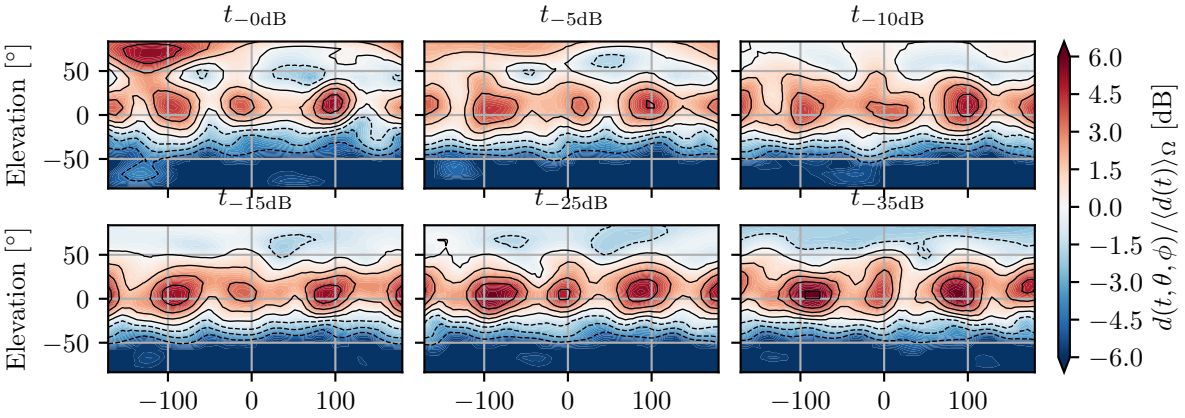

Figure 5. Normalized DEDC for the room with absorber and without diffuser panels. Figures correspond to time instances with a omnidirectional energy decay of $[0, 5, 10, 15, 25, 35]$ dB, respectively.

that the decrease in the isotropy is caused by a non isotropic sound incidence over elevation angles rather than azimuth angles, supporting the hypothesis that the decrease in the overall isotropy is caused by energy flows tangential to the absorber sample. These results seem to be in line with earlier findings by Hunt et al. [9] who found that the late decay is largely dominated by modes corresponding to a grazing incidence.

Interestingly, the isotropy estimator also predicts a decrease in the isotropy in the case of the empty room without diffuser panels (cf. Fig. 6(a)) which is likely to be caused by strong reflections from the fairly closely located floor, see Fig. 3. Again, this effect vanishes with mounted diffuser panels, cf. Fig. 2, resulting in an increased isotropy estimate, cf. Fig. 6(a). It has to be noted however, that the isotropy is very close to the maximum value of one, exhibiting the possibility that the angular resolution limit of the array and thus the estimator is reached.

The isotropy estimation has also been performed using the isotropy estimator proposed by Nolan et al. [6] which has been adapted to the DEDC for this purpose. The method yields quantitatively similar results to the method presented here. Further discussion however, is out of the scope of this paper. Nonetheless, the same set of data is also processed in [19]. Further comparisons of the two estimators are planned by the authors.

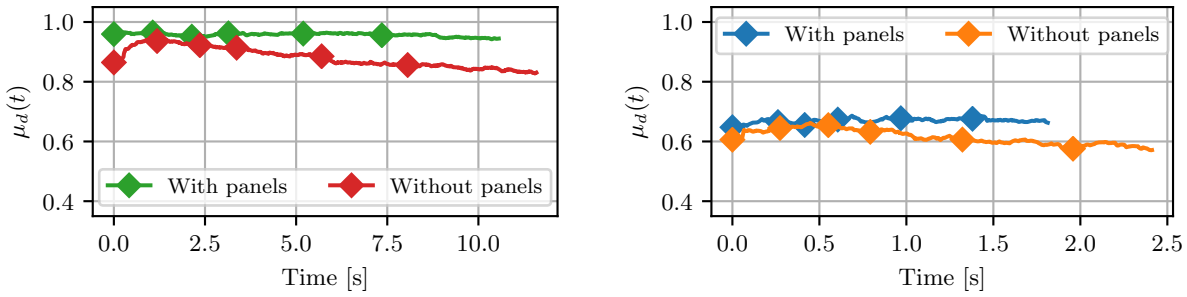

(a) Room in the empty condition.

(b) Room with absorber sample.

Figure 6. Estimated isotropy of the sound field in the 500 Hz third octave band for the four different configurations. Markers indicate a decay of $[0, 5, 10, 15, 25, 35]$ dB in the omnidirectional EDC, respectively.

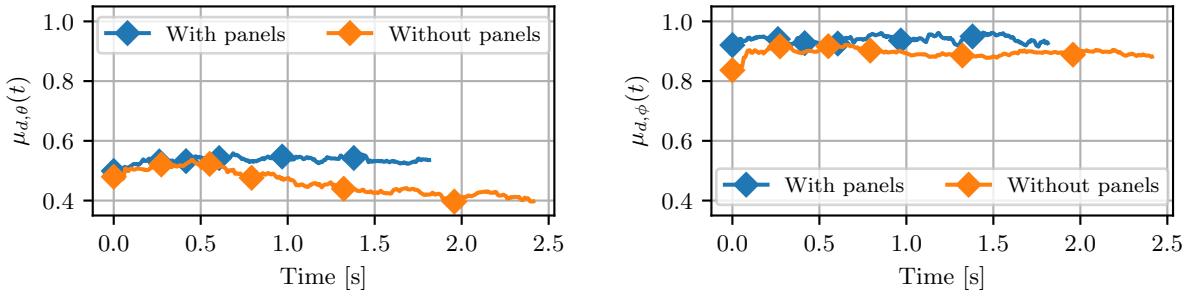

(a) Isotropy over the elevation angle.

(b) Isotropy over the azimuth angle.

Figure 7. Isotropy calculated for elevation and azimuth angles separately by first summing over the DEDC of the respective other angle. Results represent the configurations with the absorber in the 500 Hz thirds octave band. Markers indicate a decay of $[0, 5, 10, 15, 25, 35]$ dB in the omnidirectional EDC, respectively.

5 CONCLUSIONS

We presented the directional energy decay curve based on the plane wave decomposition of the sound field for the analysis of the isotropy during the decay process of the sound field in reverberation rooms. An experimental study was conducted giving insights into the directional dependence of the decaying sound field with a particular focus on the elevation angle, when an absorbing sample is placed in the reverberation room, thus clearly indicating a non isotropic sound field. Further, it was shown that the isotropy of the sound field may even decrease over time during the decay process in a rectangular room without diffuser elements due to an increased energy flow tangential to the absorber. We expect that the presented analysis method may give new insights into the well known inconsistencies in the measurement of the absorption coefficient [2].

ACKNOWLEDGEMENTS

The authors would like to thank Samuel A. Verburg for his help with the robot as well as everyone involved in helping with the experimental setup. Work presented here was funded under DFG Grant VO 600 41-1.

REFERENCES

[1] International Organization for Standardization. *ISO 354:2003 - Measurement of Sound Absorption in a Reverberation Room*. Geneva, Switzerland, 2003.

[2] R. E. Halliwell. "Inter-laboratory Variability of Sound Absorption Measurement". In: *The Journal of the Acoustical Society of America* 73.3 (Mar. 1983), pp. 880–886.

[3] H. Kuttruff. *Room Acoustics*. 4th Ed. Taylor & Francis, 2009.

[4] D. T. Bradley, M. Mueller-Trapet, J. R. Adelgren, and M. Vorlaender. "Effect of Boundary Diffusers in a Reverberation Chamber: Standardized Diffuse Field Quantifiers". In: *The Journal of the Acoustical Society of America* 135 (2014), pp. 1898–1906.

[5] F. Jacobsen and T. Roisin. "The Coherence of Reverberant Sound Fields." In: *The Journal of the Acoustical Society of America* 108.1 (2000), pp. 204–210.

[6] M. Nolan, E. Fernandez-Grande, J. Brunskog, and C.-H. Jeong. "A Wavenumber Approach to Quantifying the Isotropy of the Sound Field in Reverberant Spaces". In: *The Journal of the Acoustical Society of America* 143.4 (Apr. 2018), pp. 2514–2526.

[7] B. N. Gover, J. G. Ryan, and M. R. Stinson. "Measurements of Directional Properties of Reverberant Sound Fields in Rooms Using a Spherical Microphone Array". In: *The Journal of the Acoustical Society of America* 116.4 (2004), pp. 2138–2138.

[8] R. Thiele. "Richtungsverteilung und Zeitfolge der Schallrückwürfe in Räumen". In: *Acta Acustica united with Acustica* 3.4 (1953), pp. 291–302.

[9] F. V. Hunt, L. L. Beranek, and D. Y. Maa. "Analysis of Sound Decay in Rectangular Rooms". In: *The Journal of the Acoustical Society of America* 11.1 (July 1939), pp. 80–94.

[10] H. Kuttruff. "Eigenschaften und Auswertung von Nachhallkurven". In: *Acta Acustica united with Acustica* 8.4 (1958), pp. 273–280.

[11] M. R. Schroeder. "New Method of Measuring Reverberation Time". In: *The Journal of the Acoustical Society of America* 37.6 (1965), pp. 1187–1187.

[12] B. Rafaely. "The Spherical-Shell Microphone Array". In: *IEEE Transactions on Audio, Speech and Language Processing* 16.4 (2008), pp. 740–747.

[13] M. Berzborn, R. Bomhardt, J. Klein, J.-G. Richter, and M. Vorländer. "The ITA-Toolbox: An Open Source MATLAB Toolbox for Acoustic Measurements and Signal Processing". In: *Proceedings of the 43rd Annual German Congress on Acoustics*. DAGA. Kiel, 2017, pp. 222–225.

[14] P. Leopardi. "A Partition of the Unit Sphere into Regions of Equal Area and Small Diameter". In: *Electronic Transactions on Numerical Analysis* 25.12 (2006), pp. 309–327.

[15] G. Chardon, W. Kreuzer, and M. Noisternig. "Design of Spatial Microphone Arrays for Sound Field Interpolation". In: *IEEE Journal of Selected Topics in Signal Processing* 9.5 (2015), pp. 780–790.

[16] A. Politis and H. Gamper. "Comparing Modeled and Measurement-Based Spherical Harmonic Encoding Filters for Spherical Microphone Arrays". In: *2017 IEEE Workshop on Applications of Signal Processing to Audio and Acoustics*. WASPAA. New Paltz, NY: IEEE, Oct. 2017, pp. 224–228.

[17] N. Sneeuw. "Global Spherical Harmonic Analysis by Least-Squares and Numerical Quadrature Methods in Historical Perspective". In: *Geophysical Journal International* 118.3 (Sept. 1994), pp. 707–716.

[18] W. T. Chu. "Comparison of Reverberation Measurements Using Schroeder's Impulse Method and Decay-curve Averaging Method". In: *Journal of the Acoustical Society of America* 63.5 (1978), pp. 1444–1450.

[19] M. Nolan, M. Berzborn, and E. Fernandez-Grande. "Experimental Characterization of the Decaying Sound Field in a Reverberation Room". In: *Proceedings of the 23rd International Congress on Acoustics*. ICA. Aachen, Germany, 2019.